Microfluidics for Multiplexing of Core Needle Biopsies

Wilfrido D. Mojica[1], Kwang Oh[2], Xiaozheng Xue[3] and Edward P. Furlani[2, 3]

1 Department of Pathology and Anatomical Sciences, School of Medicine and Biological Sciences, University at Buffalo, 100 High Street, Buffalo, NY Email: mojica@buffalo.edu
2 Dept. of Electrical Engineering, University at Buffalo SUNY, Buffalo, NY
3 Dept. of Chemical and Biological Engineering, University at Buffalo SUNY, Buffalo, NY

ABSTRACT

Minimally invasive biopsies are increasingly used to obtain tissue for diagnostic purposes. The small size of these specimens can limit mutiplexed (e.g., cytologic and molecular) diagnosis as the sample is often exhausted during a single stage of analyss, e.g., cytologic analysis, which precludes subsequent molecular testing. In this presentaion we introduce a novel mocrofluidics-on-a-slide approach that combines the concepts of cytology, microfluidics and magnetophoresis to enable multiplexing of diagnostic cells. This approach emphasizes cytology for diagnostic purposes and allows recovery of the same intact cells for downstream molecular studies. In contrast to traditional approaches that sequentially partition tissue for different studies, the proposed process allows for the interrogation of diagnostic cells by different modalities, thereby enabling extraction of a maximal amount of informative data from the cells.

Keywords: core needle biopsies, mutiplexed diagnosis of core needle biopsies, microfluidics-on-a-slide, lab-on-a-slide, cytology and molecular diagnosis of core needle biopsies.

1 INTRODUCTION

Core needle biopsies (CNB) have emerged as an attractive and viable alternative to open biopsies when tissue is needed for diagnostic purposes. In contrast to an open biopsy, a CNB is less invasive, more cost efficient and can be performed on an outpatient basis [1-4]. Using image guidance, a CNB can be used to sample almost any organ site for suspicious mass lesions. Once procured, the tissue from a CNB is typically fixed in formalin, embedded in paraffin wax, sectioned and placed on glass slides. The tissue is then stained with hematoxylin and eosin for microscopic examination. Ancillary testing can be added in the form of immuno-histochemistry for the classification and even sub-classification of tumor type, and molecular testing for the selection of targeted therapies. This is the standard order by which diagnostic material from CNB are traditionally partitioned. However, a common dilemma that has arisen with CNB is the depletion of the tissue before molecular testing can be performed. This is due to several factors, one being the diminutive size of the CNB. The tissue from a CNB typically comes from either an 18G or 20G needle, with the resultant tissue having dimensions of usually less than 1 cm in length and 1 mm in width, after tissue processing. Adding to the difficulty in making a diagnosis from these small pieces of tissue is the amount of representative tumor tissue in the CNB. The less the amount of tumor present in the CNB, the harder it is to make a diagnosis. Another issue with tissue loss is waste associated with microtome effacement. Finally, the most significant depletion of tissue occurs in ancillary testing by immunohistochemistry [5-7].

In this paper, a method is introduced that enables a multiplexed approach to the evaluation of a CNB. This involves the dissociation of cells from the tissue, then enrichment of targeted cells using immunomagnetic beads followed by temporary immobilization in a microfluidic platform that is integrated on a conventional laboratory slide (microfluidics-on-a-slide) as illustrated in **Fig. 1**. This step allows for the evaluation of the enriched cell population for cytologic diagnosis. Thereafter the same cells can be recovered and assays can be performed on them. This is in contrast to the conventional approach for CNB, where the tissue is serially partitioned for separate tests. The clinical diagnosis rendered from tissue processed in the propsed approach results in the combined assessment of the cytologic impression of the cells and their molecular findings.

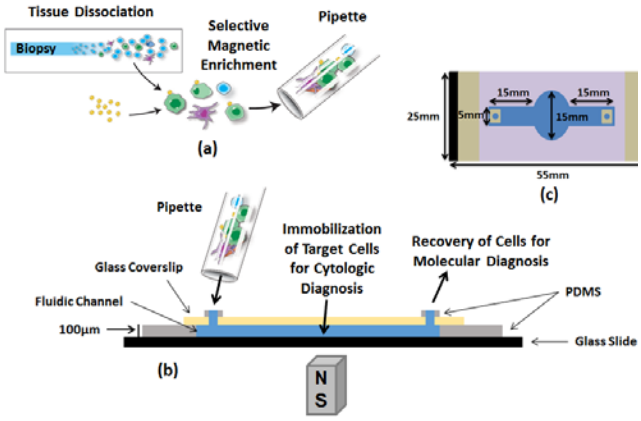

Figure 1. Diagramatic flow for processing of cytology specimens using lab-on-a-slide system: (a) processing of core needle biopsy and enrichment of target cells with immunomagnetic beads, (b) introduction of target cells via pippette into microfluidic system integrated on the top of a conventional glass slide, magnet postioned below the slide to immobilze target cells for cytologic diagnosis, (c) top viw of microfluidic system with dimensions.

2 MICROFLUIDICS-ON-A-SLIDE

The microfluidics-on-a-slide system is shown in **Fig. 2**. It was fabricated using a soft lithography technique [8-10]. To form the microchannel, a negative photoresist (MicroChem, SU-8 2050) was spin-coated on a silicon wafer substrate and patterned using a conventional photolithography technique.

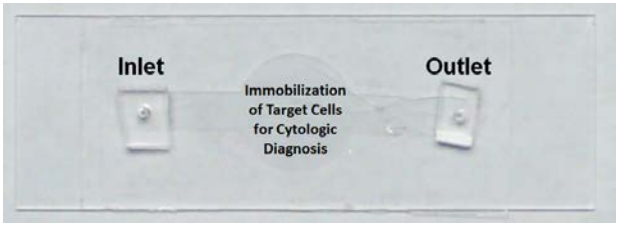

Figure 2. Fabricated microfluidc system on a glass slide.

The substrate was then silanized with hexamethyldisilazane in a vacuum chamber at room temperature for 30 minutes. This facilitated peeling the cured channel from the substrate. A base polymer of polydimethylsiloxane (PDMS) and a curing agent were thoroughly mixed at a 10:1 ratio (wt/wt). The mixture was then poured on to the substrate and a glass slide was used to push away the PDMS at a ceiling of the negative photoresist patterned with the use of a mechanical clamp [11]. After curing the PDMS was peeled off from the substrate and placed on a glass slide. The PDMS channel was then irreversibly bonded to a non-adhesive, non-charged, 25 x 75 x 1 mm glass slide (Leica Biosystems, Buffalo Grove, IL) by exposing oxygen plasma on the surface of the PDMS channel and cover glass. The channel as constructed measured 4.5 cm in length, 5 mm in width and 100 um in height. In the middle of the channel was a circular region designed for viewing that measured 1.5 cm in diameter (**Fig. 1c**). The circular design was intended to allow cells to spread out thereby preventing cells from covering and obscuring other cells. Finally, a 24 x 40 mm rectangular glass coverslip was bonded on to the top of the PDMS channel. The slightly shorter length of the glass coverslip relative to the microchannel left a small gap of 2.5 mm at both ends that could be used as inlet and outlet ports.

3 MAGNETIC ANALYSIS

The microfluidic channel was designed for placement on a small base from where a permanent magnet could be reversibly positioned just beneath the glass slide corresponding to the circular 1.5 cm viewing area (**Fig. 1 c**). A high strength (grade 42N) neodymium iron boron (NdFeB) magnet, which has a maximum remnant magnetization of B_r =1.28T, was used for the experiment. The magnet is 12.7 mm (0.5 in) in length and 6.35 mm (0.25 in) in both width and height. The magnet produces a nonuniform field distribution that induces an attractive force on magnetic particles within the microchannel. The magnet is made from grade 42N neodymium iron boron (NdFeB), which has a maximum remnant magnetization of B_r = 0.92

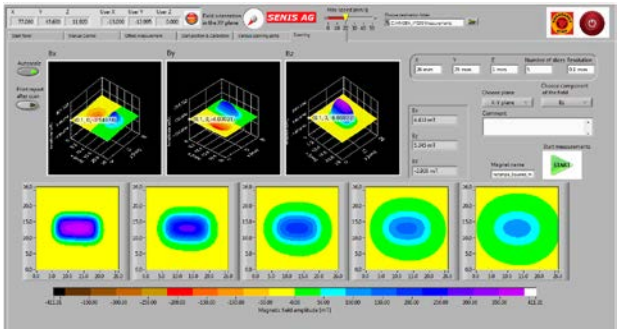

Figure 3. Measured field data from the SENIS 3D magnetic field mapping system. The three plots in the top panel are (from left to right) the spatial distribution of the field components B_x, B_y and B_z over a 26 mm × 26 mm area at a distance z = 0 mm above the magnet. The bottom panel (from left to right) contains plots of B_{total} over a 26 mm × 26 mm area at distance z = 0, 1, 2 ,3 and 4 mm, from left to right respectively.

T. The magnetic field was characterized using a 3D magnetic field mapping instrument, the MMS-1-R from SENIS GmbH (www.senis.ch) as shown in **Fig. 3**. The field distribution and force on the particles were also analysed using custom developed computational models developed using methods described by Xue and Furlani [12-15]. The force on the particles is predicted using an "effective" dipole moment approach in which a magnetized particle is replaced by an "equivalent" point dipole with a moment $\mathbf{m}_{p,eff}$. The force is given is given by

$$\mathbf{F}_m = \mu_f \left(\mathbf{m}_{p,eff} \bullet \nabla\right)\mathbf{H}_a \qquad (1)$$

where μ_f is the permeability of the fluid and $\mathbf{H}_a$ is the applied magnetic field intensity at the centre of particle. The particles used in this experiment were the Dynabeads M-450 particles (4.5 µm in diameter) from CELLection™ Epithelial Enrich Dynabeads®. A surface plot of the predicted downward axial force on the particles at a distance z = 1 mm above the magnet (at the bottom of the channel) is shown in **Fig. 4**.

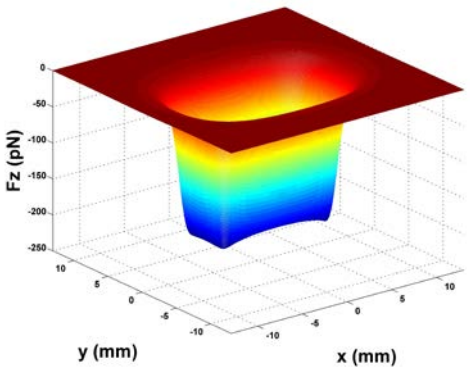

Figure 4. Surface plot of axial force F_z at z = 1 mm above the magnet.

4 MULTIPLEXED DIAGNOSIS

4.1 Sample Preparation

Thin strips of non-transformed colonic mucosa were excised from excess regions of segmental colonic resection specimens extirpated for medically indicated purposes. Colonic tissue was selected for testing based on the availability at our institution and the columnar shape of the cells. The strips of tissue were cut to approximately 2 mm in width and 1 cm in length and fixed in 25% ethanol for 2 hours. After two hours, the cells were dissociated from the tissue using the gentleMACS™ Dissociator (Miltenyl Biotec, San Diego, CA). The dispersed cell solution was filtered through Shandon™ Nylon Biopsy Bags (ThermoFischer Scientific, Waltham, MA) that allows single cells and small groups of cells to filter through, while retaining larger stromal tissue fragments. The filtered cells were then transferred to a 1.5 ml microcentrifuge tube and spun down using a table-top minifuge. The supernantant was discarded and replaced with a 1X PBS solution with 0.1% bovine serum albumin and 5 ul of resuspended CELLection™ Epithelial Enrich Dynabeads® (Life Technologies, Grand Island, NY) that had the ber-Ep4 antibody bound to them. The cells and immunomagnetic beads were incubated together at room temperature for 20 minutes with gentle mixing. The mixture was then placed in a Dynal MPC®-S magnetic particle separator for 5 minutes and the unbound cells decanted. The retained cells were stained with a 0.025% concentration of toluidine blue diluted from an originating 1% solution. The cells and stain were allowed to mix with gentle rotation. After 15 minutes, the microcentrifuge tube was spun down using the minifuge and the majority of the supernatant removed. A small amount of fluid was retained with the cells so as to be able to resupend them for eventual insertion into a microfluidic channel.

4.2 Cytologic Characteristics

Dissociation of cells from the slivers of colonic tissue resulted in single cells and small groups of cells. Immunomagnetic beads did not bind to every colonic epithelial cell. Some cells not bound to immunomagnetic beads were present in the platform immobilized with cells attached to immunomagnetic beads. Magnetophoresis was needed as a means to capture cells and immobilize them in the viewing area for cytologic examination. The small size of the immunomagnetic beads did not hinder the examination of the immobilized cells. Visual examination of the cells showed them to be almost completely columnar epithelial in nature, compatible with them being derived from the colon. The cells of interest retained their morphology as colonic epithelial cells, i.e., they remained columnar in shape with the nucleus oriented towards one pole. Dissociation from tissue, being bound to immunomagnetic beads and travelling through the microchannel did not damage the majority of cells. Staining using the supravital stain was adequate to enable evaluation of the cytologic features of the cells in the microfluidic system as shon in **Fig. 5**. There was no artifactual change in their appearance, e.g., increase in nuclear to cytoplasmic ratio or coarsening of nuclear chromatin, that would cause diagnostic confusion with malignancy.

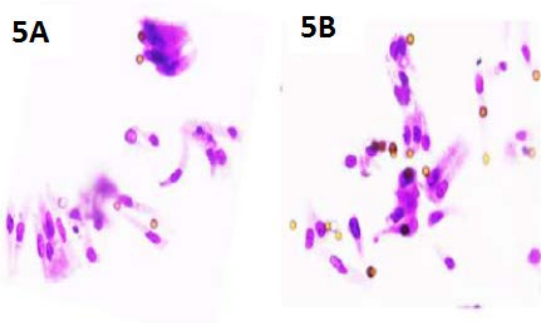

Figure 5. Two separate images of temporarily immobilized cells in the microfluidic platform's viewing stage. Cells are of colonic epithelial origin, and demonstrate preservation of columnar shape, nuclear polarity towards one pole and clear nuclear detail. Magnification 20X.

4.3 Nucleic Acid Integrity

DNA recovered from the cells was measured with A260/280 values of 1.84 and 1.87. The DNA recovered after having been fixed with ethanol and stained with the supravital dye toluidine blue could be amplified. Neither of these external factors inhibited or prevented the polymerase enzyme, which sometimes occurs with FFPE tissue. Long segments of nucleic acids measuring 1.3 and 8.5 kb could be amplified using protocols specific for long segment DNA (**Fig. 6**).

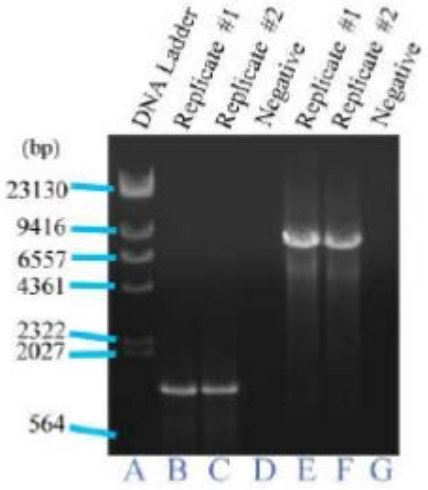

Figure 6. PCR on DNA from cells recovered from the microfluidic platform. Image demonstrates the ability to amplify long segments of DNA (1.3 kb in lanes B and C, and 8.5 kb in lanes E and F) from the recovered DNA, indicating the presence of high quality, intact, high molecular weight DNA.

5 CONCLUSION

We have introduced a mcirofluidics-on-a-slde approach for the multiplexed diagnostics of to core needle biopsies. Our results demonstrate the feasibility of using this approach for sequantial cytologic and molecular analysis. The proposed technique has several advantages relative to the conventional Formalin Fixed Paraffin Embedded (FFPE) processing approach currently practiced by virtually all pathology laboratories. Specifically, this microfluidic approach enables the multiplexing of different assays on the same cells, in contrast to the sequential partitioning of tissue sections from a CNB for different tests. Also, given a limited starting material, the ability to perform evaluations of different formats using the same diagnostic cells decreases the possibility that they are depleted before testing can be performed on them. Significantly, although we concentrated on evaluating only the elements of cytology and DNA, the recovery of intact cells would allow for the examination of other cellular components such as protein, RNA and metabolites.

ACKNOWLEDGEMENTS

The authors acknowledge financial support from the U.S. National Science Foundation, through award number CBET-1337860.

REFERENCES

[1] Yamagami, T., Ilda S., Kato, T., Tanaka, O., Kato, D., Nishimura, T. Usefulness of new automated cutting needle for tissue-core biopsy of lung nodules under CT fluoroscopic guidance. Chest. 124:147-154 (2003).

[2] Golub, R.M., Bennett, C.L., Stinson, T., Venta, L., Morrow, M. Cost minimization study of image guided core biopsy versus surgical excision biopsy for women with abnormal mammograms. J Clin Oncol. 22:2430-37 (2004).

[3] Williams, R.T., et al. Needle versus excisional biopsy for noninvasive and invasive breast cancer. Report from the national Cancer Data Base, 2003-2208. Ann Surg Oncol. 18:3802-3810 (2011).

[4] Gupta, S., et al. Quality improvement guidelines for percutaneous needle biopsy. J Vasc Interv Radiol. 21:969-975 (2010).

[5] Handorf, C.R., et al. A multicenter study directly comparing the diagnostic accuracy of expression profiling and immunohistochemistry for primary site identification in metastatic tumors. Am J Surg Pathol. 37:1067-1075 (2013).

[6] Thunnissen, E., et al. The challenge of NSCLC diagnosis and predictive analysis on small samples. Practical approach of a working group. Lung Cancer. 76:1-18 (2012)

[7] Travis, W.D., et al. Diagnosis of lung cancer in small biopsies and cytology: implications of the 2011 International Association for the Study of Lung Cancer/American Thoracic Society/European Respiratory Society classification. Arch Pathol Lab Med. 137:668-684 (2013).

[8] Lee, H., Lee, K., Ahn, B., Oh, K.W. A new fabrication process for SU-8 thick photoresist structures by simultaneously removing edge-bead and air bubbles. J Micromechanics Microengineering. 21:paper 125006 (2011).

[9] Lee, K., Kim, C., Ahn, B., Kang, J.Y., Oh, K.W. Hydrodynamically focused particle filtration using an island structure. Biochip J. 3:275-280 (2009).

[10] Ahn, B., Lee, K., Lee, H., Panchapakesan, R., Oh, K.W. parallel synchronization of two trains of droplets using a railroad-like channel network. Lab Chip. 11:3956-3962 (2011).

[11] Hsu, C.H., Chen, C., Folch, A. Microcanals for micropipette access to single cells in microfluidic environments. Lab Chip. 4:420-424 (2004).

[12] Furlani, E.P., Xue, X. Field, force and transport analysis for magnetic particle-based gene delivery. Microfluid. Nanofluid. 13(4), 589-602 (2012).

[13] Furlani, E.P., Xue, X. A model for predicting field-directed particle transport in the magnetofection process. Pharm. Res. 29(5), 1366-1379 (2012).

[14] Xue, X., Furlani, E.P. Template-assisted nano-patterning of magnetic core-shell particles in gradient fields. In Phys Chem Chem Phys. 16(26):13306-13317 (2014).

[15] Xue, X.; Furlani, E.P. Analysis of the Dynamics of Magnetic Core-shell Nanoparticles and Self-assembly of Crystalline Superstructures in Gradient Fields. The Journal of Physical Chemistry C. (2015).